Elastically coupled molecular motors

Andrej Vilfan, Erwin Frey and Franz Schwabl
Institut für Theoretische Physik, Physik-Department der Technischen Universität München, James-Franck-Straße, D-85747 Garching, Germany
(February 1, 2008)

We study the influence of filament elasticity on the motion of collective molecular motors. It is found that for a backbone flexibility exceeding a characteristic value (motor stiffness divided through the mean displacement between attached motors), the ability of motors to produce force reduces as compared to rigidly coupled motors, while the maximum velocity remains unchanged. The force-velocity-relation in two different analytic approximations is calculated and compared with Monte-Carlo simulations. Finally, we extend our model by introducing motors with a strain-dependent detachment rate. A remarkable crossover from the nearly hyperbolic shape of the Hill curve for stiff backbones to a linear force-velocity relation for very elastic backbones is found. With realistic model parameters we show that the backbone flexibility plays no role under physiological conditions in muscles, but it should be observable in certain *in vitro* assays.

I. INTRODUCTION

Molecular motors play a key role in a variety of biological processes like muscle contraction, intracellular transport, cell locomotion, flagellar rotation etc. [1]. Despite structural similarities, motors can be classified into two groups according to their function. Processive motors [2], also called "porters" [3], consist of a single molecule which can move over long distances along its molecular track without dissociating from it. The most common processive motor is kinesin interacting with microtubules. Nonprocessive motors, also called "rowers", can only generate macroscopic motion when operating in large groups. Muscular myosin, interacting with actin, belongs to this class of motors. Here we focus on nonprocessive motors.

For many decades exclusively data from physiological measurements on muscles [4] provided experimental information for modeling collective molecular motors [5,6]. In recent years, a variety of *in vitro* experimental techniques allowed the observation of single motor proteins. These experiments include gliding assays [7,8], optical tweezers [9,10] and micromechanical force measurements [11]. They allowed for a new insight into the basic principles underlying the operation of motors. Not only new theoretical models for single-molecule motors [12–15] were inspired by these experiments, but also new models for cooperative motors [3,16,17]. Except for the work by Csahók et al. [18], which discusses the transport of elastically coupled particles driven by colored noise, all these models deal with motors placed on a rigid backbone, interacting with a rigid track.

The assumption of stiff filaments seems to be appropriate under physiological conditions in muscles, since the measured extensions of few nanometers [19–21] are sufficiently small compared to the myosin step-size, which is about 10 nm [22]. However, it certainly can become invalid in gliding assays of the type discussed in Refs. [7,23] if an actin filament glides over widely separated linearly placed motors. If the spacing between motors is large enough, the elasticity of the backbone or track section between two motors can become comparable to the elasticity of a single motor head. Experiments with myosin molecules bound to an elastic background are conceivable as well.

It is the purpose of this paper to investigate qualitatively and quantitatively the influence of filament elasticity on the operation of myosin-like motors. Our major quantity of interest is the force-velocity-relation (filament velocity as a function of the external load). We want to identify the universal effects of filament elasticity and at the same time keep the model as close as possible to experiments. The elasticity modeled by linear harmonic springs may either originate from the flexible backbone or from the flexible track (Fig. 1). As long as we are dealing with small relative elongations, both sources of flexibility are equivalent and our model should apply to both cases. For specificity we use a formulation with an elastic backbone and a stiff track.

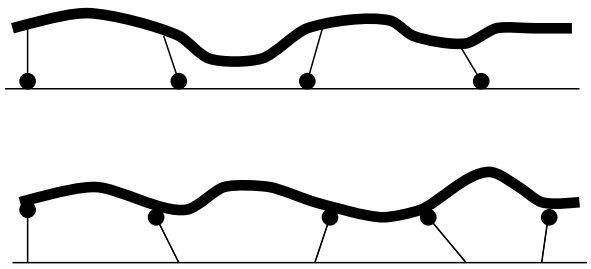

FIG. 1. Two possible sources of elastic coupling of collective molecular motors: elastic backbone (upper figure) and elastic track (lower figure). Except for very soft backbones/tracks, the description of both models is equivalent.

Another important component of the model is the modeling of individual motor heads. Most models describe the heads by several states with different conformations and transition rates between them. Such models are based on early ideas by A.F. Huxley [5] and have later been refined in order to explain more experimental details. More recently simplified models using a two-state ratchet formalism have been developed in order to concentrate on generic features of motion generation [17]. Another class of models describing Brownian particles in ratchet potentials subject to colored noise, however, seems to be only very distantly related to motor proteins [24]. We decided to use a two-state crossbridge model, similar to the model introduced by Leibler and Huse [3], but with just two long-living states. It includes the transitions between attached and detached state and an active power stroke, which have both been identified as basic elements of the myosin motor [6,2] and also observed *in vitro* [10]. Compared to other investigations [5,3,17] our model also contains a low number of free parameters, which makes it more suitable for a study of universal aspects. Yet, adding the strain-dependence of the detachment rate, the model we use is sufficient to describe the experimentally measured force-velocity-relation of actin/myosin in muscles [4]. A more detailed description of this two-state model can be found in Ref. [25].

Due to the generic features of such two-state models we expect that the effects discussed here should as well apply to other models which contain the same basic mechanisms of force generation, e.g. [3,17]. However, models of the type discussed in Ref. [18], which describe particles in an asymmetric periodic potential subject to a temporally correlated noise, are based on a thoroughly different driving mechanism. Therefore, one expects and actually finds a variety of disparate effects including a strong influence of the coupling strength on the velocity even without external load.

The outline of the paper is as follows. In Sec. II we introduce the model [26], describe its phenomenological properties, present the main results and discuss its implications to experiments. The full calculation for strain-independent detachment rates is shown in Sec. III and for strain-dependent rates in Sec. IV.

II. DISCUSSION

A. Description of the model

We consider a one-dimensional model describing many motors which produce force between two filaments gliding past each other. The force is generated by a conformational change ("power stroke") in the molecular motors fixed to the *backbone*, which takes place after they attach to the molecular *track* (Fig. 2). We assume that the motor proteins can be found in two states: attached to and detached from the track. This corresponds to taking into account only the two long-living states in the model used by Leibler and Huse [3]. The transitions between these two states occur stochastically. We denote the mean life time of the attached state by t_a and of the detached state by t_d. Each attached motor is described as a harmonic spring connecting its root at the backbone (position y) and its head on the track (position x). The force this motor produces between the track and the backbone is given as $k(x-y)$, with a spring constant k. Since the motor is in a forward leaning position before attachment (see Fig. 2), it attaches to the track at the point x^n, which is the position y of the root of the motor before attachment, shifted by the displacement d ("power stroke")

$$x^n = y + d\,. \tag{2.1}$$

We neglect thermal fluctuations and the discreteness of binding sites on the track. This is motivated by our recent results for rigid backbones [25], where we find that discrete binding sites (with a spacing of 5.5 nm) as well as thermal fluctuations have only a minor effect on the resulting force-velocity-relation.

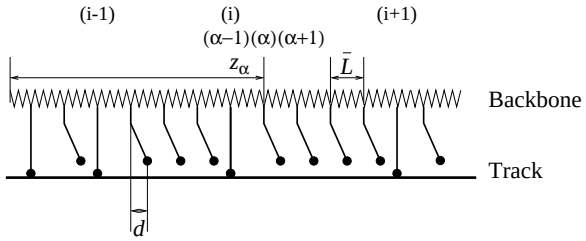

FIG. 2. Definition of the model. Motors are fixed on the elastic backbone at uniform spacing $\bar{L}$ and attach to the stiff track. z_α denotes the position of α-th motor on the unstrained backbone. Due to the conformational change, the head of each motor attaches at the distance d from its root.

While assuming a stiff track, we model the backbone as a linear spring with compliance γ^{-1} per unit length. But note that this is merely a convention. Our results apply equally well to the reverse situation, where the molecular motors are fixed on a (rigid) cover slip and the elasticity is due to the molecular track transported by them. We consider $\bar{N}$ motors placed on the backbone at uniform spacing $\bar{L}$, so that the total backbone length is $\bar{N}\bar{L}$. Note that the assumption of uniform spacing is made solely for simplicity. Any other distribution which is homogeneous on length scales L would lead to the same exponential distribution of gap widths (see Eq. 2.3 below). The position of the α-th motor on the unstrained backbone will be referred to as z_α. In the following, the actual positions of motor heads $x_\alpha(t)$ and of motor roots $y_\alpha(t)$ are measured relative to z_α (Fig. 3).

Instead of using the quantities $\bar{N}$ and $\bar{L}$ it will prove helpful to use the mean number of attached motors $N = \bar{N}t_a/(t_a+t_d)$ and the mean spacing between two

attached motors $L = \bar{L}(t_a + t_d)/t_a$. Since for now we are dealing with strain-independent reaction rates the distribution of attached and detached states does not depend on the motion of their positions. The probability of finding a gap with α detached motors between two attached ones is given by the geometric distribution

$$p_\alpha = \left(\frac{t_d}{t_a + t_d}\right)^\alpha \frac{t_a}{t_a + t_d} \,. \tag{2.2}$$

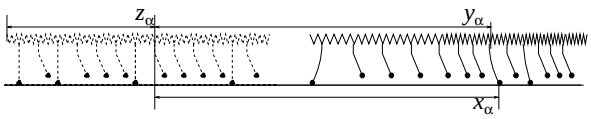

FIG. 3. The moving backbone (solid line) and its initial position at time $t = 0$ (dashed line). y_α denotes the root position of the α-th motor, relative to its initial value (z_α). x_α denotes the head position of the α-th motor, also relative to the initial position of the α-th root, z_α.

In order to keep the model as lucid as possible we assume a small duty ratio [2], meaning that a motor molecule spends most of its time in the detached state, $t_a \ll t_d$. Since we are dealing with nonprocessive motors ("rowers" [3]), this assumption is certainly valid. While keeping the mean number N of attached motors and their average spacing L constant, we consider the limit $\bar{L} \to 0$. With this simplification the model becomes continuous. Also, the assumption about equidistantly placed motors on the backbone becomes superfluous in this limit. The distribution of motors is insignificant as long as it is sufficiently homogeneous on the length scale L. The attachment rate per length L (between the positions z and $z + L$ on the backbone) obeys $r_a = L/\bar{L}t_d = 1/t_a$. The distribution of gap widths (2.2) takes the form of an exponential distribution

$$p(l) = \frac{1}{L} e^{-l/L} \,. \tag{2.3}$$

B. Results

In this subsection we summarize our main results for the analysis of the model described above; the details of the calculation are given later in Sec. III.

As described by now the model contains seven independent parameters: t_a, N, L, F, k, γ and d. Upon measuring the force per motor, F/N, in units of the force during one power stroke, kd, and measuring the backbone elasticity per unit length, γ/L, in units of the motor head elasticity, they may be reduced to two adimensional parameters: $\hat{F} = F/Nkd$ and $\hat{\gamma} = \gamma/kL$. Then the velocity in units of a single motor velocity $\hat{v} = vt_a/d$ is given by a "scaling" function $\hat{v} = \eta(\hat{F}, \hat{\gamma})$.

As shown in Sec. III we find that in case of a time-independent external force it does not matter whether this force pulls on one end or homogeneously on the whole backbone with a density $f = F/NL$. A quite remarkable result of our analysis is that the force-velocity relation remains linear for flexible backbones and that the zero load velocity d/t_a does not depend on the backbone elasticity. The force-velocity relations for a stiff and an elastic backbone are shown in Fig. 4.

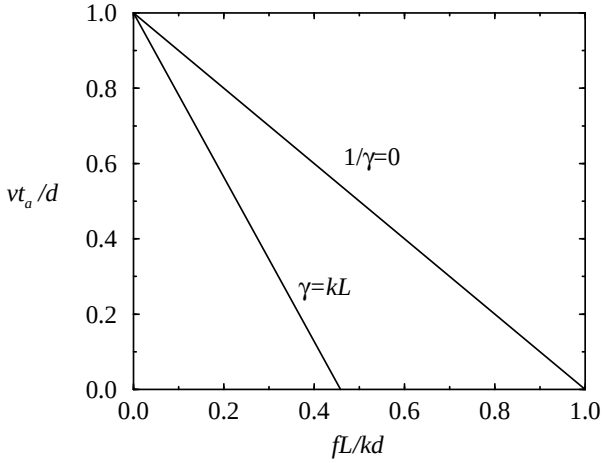

FIG. 4. Force-velocity-relation for the stiff ($\gamma = \infty$) and elastic ($\gamma = kL$) backbone.

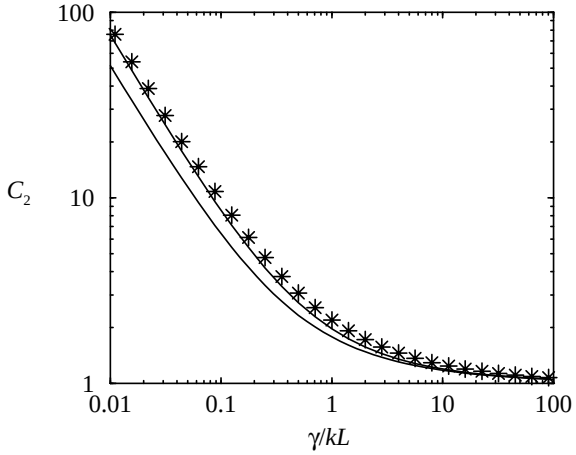

FIG. 5. The slope of the force-velocity relation (coefficient C_2 in Eq. (3.16)), as a function of the relative backbone stiffness γ/kL: MC-simulations (stars), analytic approximation without correlations (lower curve), with correlations to the distances to nearest neighbors (upper curve). In both analytic curves the numeric result for $k\langle 1/K_e\rangle$ from Fig. 9 was used.

If the relative backbone stiffness $\hat{\gamma}$ lies below 1, the slope of the force-velocity curve and consequently the

stall force differ significantly from those for a stiff backbone (Fig. 5). While the stall force $f_{\rm stall}$ is proportional to the motor stiffness ($f_{\rm stall} = kd/L$) for stiff backbones, it becomes a function of backbone stiffness for very flexible backbones and is given as $2\gamma d/\nu L^2$. Here ν is a numerical constant which has the value $\nu \approx 1.64$ as obtained from the Monte-Carlo simulation. Using analytical tools based on a Master-Equation approach with correlations between the position of a motor and the distances to its neighbors, we obtain the value $\nu \approx 1.50$, which is in good agreement. For completeness Fig. 5 also shows the result of a Master-Equation without correlations, yielding $\nu = 1$.

Finally, we extend the model described in Sec. II A by introducing a strain-dependent detachment rate. This extension is inevitable for a quantitative comparison with experiments on the actin-myosin system. We already mentioned that (with or without backbone elasticity) strain-independent transition rates lead to a linear force-velocity-relation. However, since the very beginning of muscle research it has been known that the force-velocity-relation rather has a hyperbolic form, also called the Hill curve [4]. It has also been known that the energy liberation in a stretching muscle depends on velocity, which is also called the Fenn effect [27]. The most natural way to reproduce these physiological measurements is the introduction of a strain-dependent detachment rate, meaning that the lifetime of the attached state $t_a = t_a(x_i - y_i)$ is larger for those heads that have just gone through the power stroke and produce maximum force than for those which have already done their work and now pull backwards. As a consequence the duty ratio becomes lower at higher velocities. This idea has already been used by A.F. Huxley [5]. Although there is some direct experimental evidence for strain-dependent detachment rates [10], the functional form of this dependence has not been measured yet. For simplicity we model this dependence as an exponential $t_a(\xi) = \exp(\alpha\xi)$, which suffices to fit the force-velocity-relation [4]. However, we stress that this is only a first approximation and that other forms are possible as well. Further experimental information is highly desirable for a future more detailed modeling of molecular motors.

Some other functional forms of the detachment rate (e.g. $t_a(\xi) \propto \xi^{-2}$) lead to anomalous force-velocity-relations already with rigid backbones [25]. These can lead to oscillations, similar to those proposed by Jülicher and Prost [28]. We expect that flexible backbones can lead to additional phenomena like wave generation.

Strain-dependent detachment rates enhance the difficulty of an analytic solution of our model enormously, since the distribution of attached and detached motors depends on the distribution of head positions (x_i). Therefore, we will mainly use Monte-Carlo simulations and restrict analytic arguments on limiting cases. The simulations show that two major analytic results of the strain-independent case carry over to the strain-dependent case: (i) If the backbone flexibility exceeds its characteristic value, the stall force decreases strongly. (ii) The backbone flexibility has only little influence on the zero-load velocity.

For stiff backbones ($\gamma/kL \gg 1$) the force-velocity-relation as measured by Hill [4] is reproduced perfectly using the value $\alpha d = 0.58$. For decreasing backbone stiffness ($\gamma/kL \ll 1$) the stall force decreases and the force-velocity-curve becomes increasingly linear. This can be understood as follows: The forces which lead to positive velocities become smaller and so does the strain on single motors. The small strain does not have any significant influence on the detachment rate any more and the results obtained for a strain-independent detachment rate become exact. The crossover from the Hill curve to a linear relation is shown in Fig. 6. There $\alpha d = 0.5$ is used, but the curves would look qualitatively similar for other positive values.

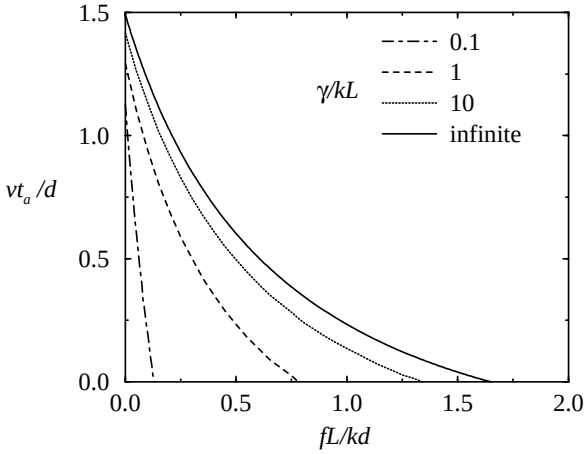

FIG. 6. Monte-Carlo results for force-velocity-relations with strain-dependent detachment rates ($\alpha d = 0.5$) and different backbone stiffnesses. Note the crossover from the Hill curve at stiff backbones to a nearly linear relation at soft backbones.

C. Implications for experiments

In order to apply our theory to experiments, we need the spring constants of the myosin heads and of the actin filaments. The elasticity of the attached myosin head was measured by Finer et al. [22] with the result $k = 0.4\,\mathrm{pN/nm}$ (measurements by Ishijima et al. [29] yield $k = 0.28\,\mathrm{pN/nm}$, which is in quite good agreement).

In our model we assumed springs with flexibility proportional to their length, obeying $k_{\rm spring} = \gamma/L$. Actually actin is a semiflexible polymer. Its elastic behavior was subject of many theoretical and experimental studies in last years [30–34]. There are essentially two contributions to the elasticity of actin: the longitudinal elastic modulus and the buckling of the polymer, induced through thermal fluctuations.

At very high loads, the stiffness is limited by the elastic modulus of actin and is proportional to L^{-1}. For a filament of length 1 μm the stiffness is about 44 pN/nm [34]. In this regime, the characteristic distance between attached motors can be estimated as $L_{\rm ch} = \gamma/k \approx 100\,\mu$m. In this case backbone flexibility is of no experimental relevance.

At low tension, the buckling modes limit the stiffness of actin. In the linear response approximation, the stiffness of a polymer with length L obeys the law

$$k_{\rm polymer} = 90 k_B T \ell_p^2 L^{-4} \tag{2.4}$$

where ℓ_p denotes the persistence length. Although we assume springs obeying an L^{-1}-law, we can still use the L^{-4}-law to give an estimate for the characteristic distance for which $k_{\rm polymer}(L_{\rm ch}) \approx k$.

Recent measurements provide the value $\ell_p = 7.4\mu$m [35]. With these values we finally estimate the characteristic distance between attached motors $L_{\rm ch} = (90 k_B T \ell_p^2/k)^{1/4} \approx 500\,$nm. If the mean displacement between attached motors is larger than $L_{\rm ch}$, we expect that the effects of backbone elasticity should be observable. A simulation with springs obeying the L^{-4}-law (2.4) is in preparation.

In muscles 500 nm is about the length of a half sarcomere [36,1]. A rough estimate (300 myosin heads in one thick filament, 3 actin filaments per one thick filament, $2.5 - 10\%$ of heads in the attached state) leads to L values between 50 nm and 200 nm, significantly below the characteristic length $L_{\rm ch}$. This implies that the elasticity of actin filaments does not influence the operation of muscles. This result is not surprising – backbone elasticity always reduces the efficiency of motors and it would be hard to understand why muscles spoil their high efficiency in such a prodigal way.

III. ANALYTICAL SOLUTION

In this section the calculation leading to the force-velocity-relation for strain-independent detachment rates is given. This is done in several steps: first we show that the model behaves equivalently if a force acts on one end of the filament or homogeneously along the whole length. As second we calculate the effective compliance of a semi-infinite chain, which is an important input quantity for later use. Then we show the linearity of the force-velocity-relation, show that the zero-load velocity does not differ from its value for stiff backbones and finally calculate its slope in two different approximations.

A generic situation found in many experimental setups is that a force F, usually produced by an optical tweezer, acts on the rear end of the backbone. Another possibility is to produce the force by a viscous liquid, flowing along the backbone. Such a force acts more or less homogeneously on the whole backbone. In both cases the main quantity of interest is the resulting mean backbone velocity depending on the load F. In the following we show that both situations are equivalent within the scope of a theoretical description.

A. Point force

From now on we use the index i, which runs over attached motors only, instead of the index α, running over all motors. x_i and y_i denote the head and root positions of i-th attached motor relative to its initial position on the unstrained backbone (z_i) at time $t = 0$. The stiffness of the backbone fragment between the motors i and $i+1$ equals $\gamma/(z_{i+1} - z_i)$. At the point where the i-th motor is fixed to the backbone, the sum of the all three forces (from the motor, from the left part of the backbone and from the right part of the backbone) must be zero:

$$k(x_i - y_i) - \gamma\frac{y_i - y_{i-1}}{z_i - z_{i-1}} + \gamma\frac{y_{i+1} - y_i}{z_{i+1} - z_i} = 0\,, \tag{3.1a}$$

$$k(x_1 - y_1) + \gamma\frac{y_2 - y_1}{z_2 - z_1} = F\,. \tag{3.1b}$$

The second equation describes the first attached motor and differs from the others since the backbone force acting from the left is replaced by the external force F. With given x_i and z_i this set of equations allows us to determine the values of y_i.

The *detachment* rate equals t_a^{-1} for each motor. The detachment of one motor is described by canceling its position in the set of x- and z-values. Afterwards, all the y-values are determined anew from Eq. (3.1).

The process of *attachment* occurs at the rate N/t_a and consists of choosing a random position z^n between 0 and NL, calculating the corresponding $y(z^n)$ (the root position of the new motor before attaching) and $x^n = y(z^n) + d$, and finally adding a new motor with its head at x^n and its root at z^n. Again, all the y-values have to be recalculated as stated by Eq. (3.1). Expressing $y(z^n)$ through the positions of the neighbors (the index "$-$" describes the first attached motor on the left and "$+$" on the right hand side) yields

$$x^n = y^n + d = \frac{y_-(z_+ - z^n) + y_+(z^n - z_-)}{z_+ - z_-} + d\,. \tag{3.2}$$

B. Equivalence to the model with a homogeneous force

In the model described by now, the external force acts on one end of the backbone. This leads to some difficulties, e.g. one can only consider a semi-infinite chain with one boundary condition. Furthermore, the resulting solutions are not translationally invariant since the strain decreases along the backbone.

Replacing the point force by a homogeneous one acting on the whole backbone with a density $f = dF/dz$ would

allow us to perform the calculation on an infinite chain of completely equivalent motors. The ability to use periodic boundary conditions in the Monte-Carlo-simulation would be an additional advantage.

Fortunately, both models, i.e. with a point force and a homogeneous force are actually equivalent. It is instructive to show this equivalence in the continuum formulation of the model. Instead of the discrete set of variables y_i^P we use a function $y^P(z)$. The continuum representation of Eqn. (3.1)) is given by the following set of equations

$$\gamma \frac{d^2 y^P}{dz^2} = -\sum_i \delta(z - z_i) k(x_i^P - y^P(z_i)) \,, \tag{3.3a}$$

$$\gamma \left. \frac{dy^P}{dz} \right|_{z=0} = F \,. \tag{3.3b}$$

The first equation expresses the constant tension between the attached motors with jumps at the positions where the motor roots are placed. The second equation describes the strain at the boundary of the backbone.

On the other hand, in the homogeneous force model the strain grows linearly with z

$$\gamma \frac{d^2 y^H}{dz^2} = f - \sum_i \delta(z - z_i) k(x_i^H - y^H(z_i)) \,. \tag{3.4}$$

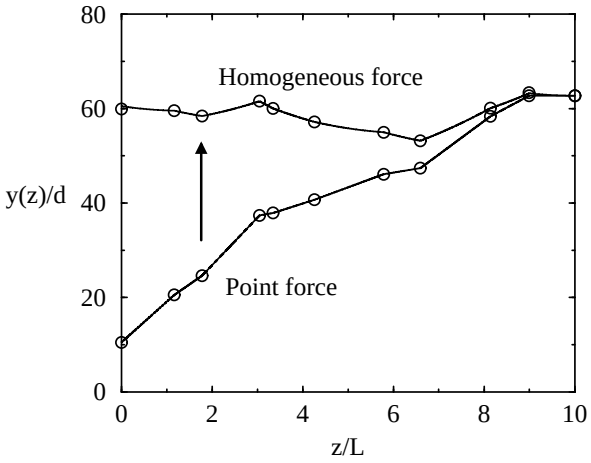

FIG. 7. Transformation from the model with a point force to the model with a continuous force, given through Eq. (3.5), on a typical configuration during the motion. The circles represent attached motors, the detached ones lie on the line. z denotes the position a motor would have on an unstrained backbone, y its root position relative to z (Fig. 3).

Since we are dealing with a force constant in time and with quasistationary solutions, we can show that both models are equivalent up to a transformation which shifts the heads and roots of motors, depending on their z position. As may be easily verified by comparing Eqns. (3.3) and (3.4), the following transformation

$$\begin{Bmatrix} x_i^H \\ y_i^H \end{Bmatrix} = \begin{Bmatrix} x_i^P \\ y_i^P \end{Bmatrix} + \frac{f}{2\gamma}(NL - z_i)^2 \tag{3.5}$$

with $F = NLf$ preserves the properties of the model. The transformation is shown schematically in Fig. 7. After having shown the equivalence of both models, we can return to the original formulation. The transformed equations (3.1) and (3.2) become (in the following we omit the index ^{H})

$$k(x_i - y_i) - \gamma \frac{y_i - y_{i-1}}{z_i - z_{i-1}} + \gamma \frac{y_{i+1} - y_i}{z_{i+1} - z_i} - f \frac{z_{i+1} - z_{i-1}}{2} = 0 \tag{3.6}$$

and

$$x^n = \frac{y_-(z_+ - z^n) + y_+(z^n - z_-)}{z_+ - z_-} + d - \frac{f}{2\gamma}(z_+ - z^n)(z^n - z_-) \,. \tag{3.7}$$

The additional term represents the displacement of a uniformly loaded spring, tightly bound at its ends at z_- and z_+. Of course, these equations also follow directly from (3.4).

C. Effective compliance of a semi-infinite chain

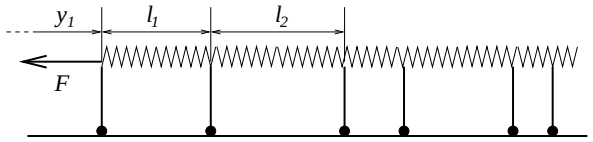

FIG. 8. Effective spring constant of a semi-infinite chain with randomly distributed displacements between bridges.

A quantity frequently needed during the analytical solution of the model described in Sect. II is the elasticity of a semi-infinite stochastic chain as shown in Figure 8. It is defined as

$$\frac{1}{K_e} = -\left. \frac{dy_1}{dF} \right|_{x_i = \text{const}} \tag{3.8}$$

where y_1 is a part of the solution of Eq. (3.1). As defined in Sect. II A, the spring constant of the motors is given by k. The values of l_i are distributed randomly with average L and the exponential distribution (2.3).

The compliance of a chain with a given configuration (given l_i-values) can be calculated recursively. The chain is built up of a spring with stiffness k, connected in parallel to two other springs, which themselves are connected in series. The first one describes the piece of backbone with elasticity γ/l_1. The second spring is again a replacement for another semi-infinite chain starting with the second motor. We denote its stiffness as K_e'.

$$K_e = k + \frac{1}{\frac{l_1}{\gamma} + \frac{1}{K_e'}} \tag{3.9}$$

Repeating the same procedure for K_e' etc. and finally averaging over all configurations $(l_1, l_2, \ldots)$ with their statistical weights yields

$$\left\langle \frac{1}{K_e} \right\rangle = \int_0^\infty dl_1 p(l_1) \int_0^\infty dl_2 p(l_2) \ldots \frac{1}{k + \cfrac{1}{\frac{l_1}{\gamma} + \cfrac{1}{k + \cfrac{1}{\frac{l_2}{\gamma} + \cfrac{1}{k + \frac{1}{\ldots}}}}}} \; . \tag{3.10}$$

The convenient way to solve this high-dimensional integral, however, is by using the Monte-Carlo method. Its result is shown in Fig. 9.

One possibility to give an analytic approximation for $\left\langle K_e^{-1} \right\rangle$ is the use of a mean-field like theory by assuming that all displacements l_i are exactly equal to their mean value L. Then the above expression becomes self-similar and we obtain the recursion relation

$$\left\langle \frac{1}{K_e} \right\rangle = \frac{1}{k + \frac{1}{\frac{L}{\gamma} + \left\langle \frac{1}{K_e} \right\rangle}} \tag{3.11}$$

with the solution

$$\left\langle \frac{1}{K_e} \right\rangle = \frac{L}{2\gamma} \left(\sqrt{1 + 4\frac{\gamma}{kL}} - 1 \right) \; . \tag{3.12}$$

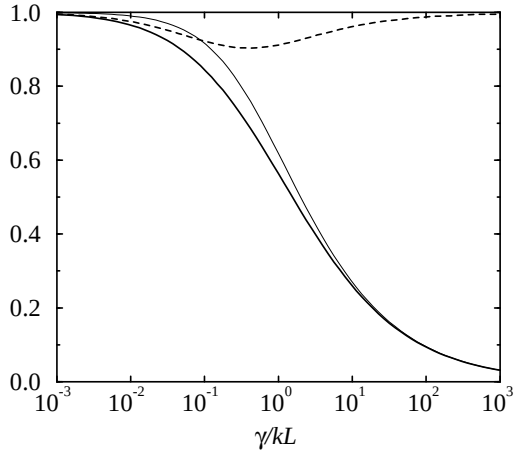

FIG. 9. The effective compliance of a semi-infinite chain $k\langle 1/K_e \rangle$. Thick line: Monte-Carlo result. Thin line: approximation given by Eq. (3.12). Dashed line: the ratio between the Monte-Carlo result and the approximation.

In Fig. 9 the approximation, Eq. (3.12) is plotted against the (exact) Monte-Carlo solution of (3.10). The deviations lie below 10% over the entire parameter range. The approximation becomes exact for both very soft and very rigid backbones. In the case of large γ this is due to the fact that the long-range coupling makes the detailed distribution of l_i irrelevant. The case of low γ is trivial since the motors get decoupled and the stiffness of the chain is determined solely by the first motor ($\left\langle K_e^{-1} \right\rangle = \frac{1}{k}$).

D. Linearity of the force velocity relation

For rigidly coupled motors it was already shown in [3] that the velocity is linear in the applied force f as well as in the step size d. In the following we present a simple argument why this remains valid for elastically coupled motors. We denote the number of currently attached motors by n and their positions on the backbone by a vector $\mathbf{x}$ containing the components $x_1 \ldots x_n$. From the structure of Eqns. (3.6) and (3.7) it is evident that the process of attachment can be described by the following equation

$$\mathbf{x}^{(i+1)} = A\mathbf{x}^{(i)} + \mathbf{u}_1 \frac{fL}{k} + \mathbf{u}_2 d \tag{3.13}$$

where the $(n+1, n)$-matrix A and the $(n+1)$-vectors $\mathbf{u}_1$ and $\mathbf{u}_2$ depend in a complex way on $\{z_i\}$ and γ/Lk. The detachment of one head is described by another $(n-1, n)$-matrix A as

$$\mathbf{x}^{(i+1)} = A\mathbf{x}^{(\mathbf{i})} \; . \tag{3.14}$$

After a series of consecutive attachments and detachments this gives

$$\mathbf{x}^{(i)} = \tilde{A}\mathbf{x}^{(0)} + \tilde{\mathbf{u}}_1 \frac{fL}{k} + \tilde{\mathbf{u}}_2 d \; . \tag{3.15}$$

Finally we set $\mathbf{x}^{(0)} = 0$ and calculate the mean motor position $\langle x \rangle = \mathrm{tr}\, \mathbf{x}/n$. Since the time needed for i steps is proportional to t_a, we obtain the relation

$$v = \frac{1}{t_a} \left(C_1 d - C_2 \frac{fL}{k} \right) \; , \tag{3.16}$$

which is linear in d and in f. The constants C_1 and C_2 get independent of the mean number of motors N for $N \to \infty$.

The force-velocity-relations for the elastic and for the stiff backbone are compared in Fig. 4. Due to the linearity of the force-velocity relation the problem can be separated in two parts: determining the backbone velocity without external forces ($f = 0$) and the velocity with external force but without power strokes ($d = 0$). The remaining work consists of determining the constants C_1 and C_2.

E. Master-equation

An adequate description of the model is given by $P(\ldots, l_2, l_1; x, t; r_1, r_2, \ldots)$, the probability density to find a head at position x and with distances $l_1 \equiv z_i - z_{i-1}$ and $r_1 \equiv z_{i+1} - z_i$ to its nearest attached neighbors, the distances $l_2 \equiv z_{i-1} - z_{i-2}$ and $r_2 \equiv z_{i+2} - z_{i+1}$ between the nearest and the next nearest attached neighbors etc.. Of course, this distribution varies with time. Because the problem is linear in x and y, there is no need for determining the correlations between the positions of different motor heads on the track. P can be expressed by

$$P(\ldots, l_2, l_1; x, t; r_1, r_2, \ldots) = P(x,t)_{\ldots, l_2, l_1; r_1, r_2, \ldots} p(\ldots, l_2, l_1; r_1, r_2, \ldots) \; . \tag{3.17}$$

The second factor describes the probability for a motor to have the distances l_1, r_1, l_2, r_2, ... to its neighbors. In a steady solution it is given by Eq. (2.3)

$$p(\ldots, l_2, l_1; r_1, r_2, \ldots) = \frac{e^{-l_1/L}}{L} \frac{e^{-r_1/L}}{L} \frac{e^{-l_2/L}}{L} \ldots \tag{3.18}$$

The first factor gives the distribution of the head positions x for the given set of distances. Since the transition rates are constant (strain-independent), the first factor does not influence the second one.

We describe the temporal development of P in terms of a Master equation. The detachment of motors is described as drain, attachment as source. Additional terms result from the fact that the attachment/detachment of a motor also changes the l and r-values in its neighborhood.

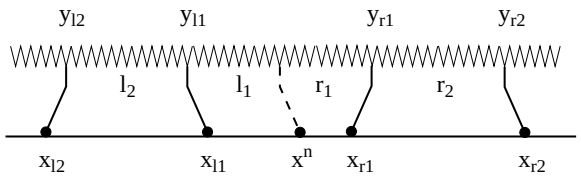

FIG. 10. Attachment of a new head.

The detachment rate is equal to the probability density divided through the mean life time of the attached state

$$r_d(\ldots, l_2, l_1; x, t; r_1, r_2, \ldots) = \frac{1}{t_a} P(\ldots, l_2, l_1; x, t; r_1, r_2, \ldots) \; . \tag{3.19}$$

Once the distribution of z-values ($p(\ldots, l_2, l_1; r_1, r_2, \ldots)$) is in equilibrium, the attachment and detachment rate integrated over x have to be equal. They can only differ in the x-dependence. Thus we write the attachment rate the same way as the detachment rate except for a different factor containing the distribution of x-positions of the newly attached heads.

$$r_a(\ldots, l_2, l_1; x, t; r_1, r_2, \ldots) = \frac{1}{t_a} p(\ldots, l_2, l_1; r_1, r_2, \ldots) P^n(x,t)_{\ldots, l_2, l_1; r_1, r_2, \ldots} \tag{3.20}$$

The x-distribution of attaching motors depends on the x-distributions of all the neighbors. It is determined as the integral over all (properly weighted) configurations which lead to a motor attachment at position x^n:

$$P^n(x,t)_{\ldots, l_2, l_1; r_1, r_2, \ldots} = \ldots \int dx_{l1} P(x_{l1}, t)_{\ldots, l_3, l_2; l_1, r_1 \ldots} \int dx_{r1} P(x_{r1}, t)_{\ldots, l_1, r_1; r_2, r_3 \ldots} \ldots \delta\left(x^n(\ldots, x_{l1}, x_{r1}, \ldots) - x\right) \tag{3.21}$$

As follows form Eq. (3.7), x^n can be expressed through y_{l1} and y_{r1}

$$x^n = \frac{y_{l1} r_1 + y_{r1} l_1}{l_1 + r_1} + d - \frac{f}{2\gamma} l r \; , \tag{3.22}$$

which again are functions of all x_i and can be determined through Eq. (3.6). The full Master equation is given in Appendix A.

F. Zero load backbone velocity

In the special case of zero external load ($f = 0$) one can see that as long as the expectation value $\langle x \rangle_{\ldots, l_2, l_1; r_1, r_2, \ldots}$ is independent of the distances l_i and r_i, i.e.

$$\int dx \, x \, P(x,t)_{\ldots, l_2, l_1; r_1, r_2, \ldots} = \langle x \rangle \; , \tag{3.23}$$

the same holds for y_i (determined from (3.6)) and for x^n, which follows from Eq. (3.22)

$$\langle x^n \rangle = \langle y \rangle + d = \langle x \rangle + d \; . \tag{3.24}$$

In other words, if the average head position of the existing attached motors is not correlated to the distances between them, the position where the head of a new motor attaches is uncorrelated too. Thus we have shown self-consistently that $\langle x \rangle_{\ldots, l_2, l_1; r_1, r_2, \ldots}$ does not depend on l_i and r_i. The equation of motion (A2) for the expectation value of x simplifies to

$$v \equiv \frac{d}{dt}\langle x\rangle = \frac{1}{t_a}\left(\langle x^n\rangle - \langle x\rangle\right) = \frac{d}{t_a}\,. \tag{3.25}$$

This means

$$C_1 = 1 \tag{3.26}$$

for the first coefficient in Eq. (3.16). The interesting point in this result is that it is independent of the backbone elasticity. As long as there is no external force, the velocity remains the same as in the case of a rigid backbone, this is $v(f=0) = d/t_a$.

G. Slope of the force-velocity curve (correlations neglected)

In the previous section we have shown that in the case of zero external force the average x-position of a motor stays uncorrelated to the distances to its attached neighbors, which made the calculation of the force-velocity relation pretty easy. In the case of nonvanishing external forces (behavior described by the coefficient C_2 in Eq. 3.16), the correlation doesn't vanish any more. However, as a first approximation we may still try to neglect it. Later we will take correlations with distances to the nearest neighbors into account and show that they improve the result significantly.

The solution is analog to the previous section, except that we set $d = 0$ and $f \neq 0$ in Eq. (3.22). Another difference is that the average y-value differs from the average x-value by the mean force per attached motor (fL), divided through the motor stiffness k

$$\langle y\rangle = \langle x\rangle - \frac{fL}{k}\,. \tag{3.27}$$

Instead of this rather intuitive argument this equation can also be derived directly from Eq. (3.6) by summation over i.

This equation describes the y-position, averaged over all motors. However, the quantities needed in Eq. (3.22) are the expectation values of y_{r1} and y_{l1} (motors at the edge of a gap whose distance to one neighbor is $l_1 + r_1$ and to the other neighbor randomly distributed). Even with uncorrelated x-values the expectation values $\langle y_{l1}\rangle$ and $\langle y_{r1}\rangle$ are not the same as $\langle y\rangle$.

For a gap width equal to the mean distance between attached motors both quantities will not differ. Otherwise the average value of the y-positions beneath a gap of width $l_1 + r_1$ differ from $\langle y\rangle$ by the excess force acting on the gap between them ($f(l_1 + r_1)$) compared to the force on the average gap (fL), multiplied by the effective compliance of a semi-infinite chain (Sect. III C)

$$\langle y_{l1}\rangle = \langle y_{r1}\rangle = \langle y\rangle - f\left\langle\frac{1}{K_e}\right\rangle\frac{l_1 + r_1 - L}{2} \tag{3.28}$$

The denominator 2 describes the fact that the force is distributed equally to both edges.

The mean x-position of the newly attached motor follows by combining Eqns. (3.22), (3.27), and (3.28):

$$\langle x^n\rangle_{l_1;r_1} = \langle x\rangle - f\left(\left\langle\frac{1}{K_e}\right\rangle\frac{l_1 + r_1 - L}{2} + \frac{L}{k} + \frac{l_1 r_1}{2\gamma}\right) \tag{3.29}$$

Since we want to neglect correlations between $\langle x\rangle$ and (l_i, r_i), we average over l_1 and r_1 ($\langle l_1\rangle = \langle r_1\rangle = L$)

$$\langle x^n\rangle = \langle x\rangle - f\left(\left\langle\frac{1}{K_e}\right\rangle\frac{L}{2} + \frac{L}{k} + \frac{L^2}{2\gamma}\right)\,. \tag{3.30}$$

In analogy to the previous section the final result for the dimensionless coefficient C_2 is

$$C_2 = \left(\frac{k}{2}\left\langle\frac{1}{K_e}\right\rangle + 1 + \frac{kL}{2\gamma}\right)\,. \tag{3.31}$$

The result is shown in Figure 5. In the limit of very soft backbones ($\gamma \ll kL$) the stall force becomes $f_{\text{stall}} = 2d\gamma/L^2$, which is independent of the motor stiffness k. Our Monte-Carlo simulations show this behavior, however with a different prefactor, which results from the correlations which were neglected in this approximation,

$$f_{\text{stall}} = \frac{2d\gamma}{\nu L^2} \tag{3.32}$$

with $\nu \approx 1.64$.

H. First-order correlations

Contrary to the previous subsection where we neglected the correlation between the position x of a motor and the distances to its neighbors by using the ansatz (3.23), we now extend the calculation by taking correlation with distances to nearest neighbors into account. We replace the approximation (3.23) by introducing a function describing these correlations

$$\int dx\, x\, P(x,t)_{\ldots,l_2,l_1;r_1,r_2,\ldots} = \langle x(t)\rangle - \frac{fL}{k}\mu\left(\frac{l_1}{L};\frac{r_1}{L}\right)\,. \tag{3.33}$$

The function μ is scale invariant. It has to fulfill the condition

$$\int dl_1 \int dr_1 p(l_1;r_1)\mu\left(\frac{l_1}{L};\frac{r_1}{L}\right) = 0\,. \tag{3.34}$$

This also means that the head positions of the motors limiting a gap of width $l_1 + r_1$ already differ from $\langle x\rangle$

$$\langle x\rangle_{l_1+r_1;} = \langle x\rangle - \frac{fL}{k}\int_0^\infty dr_2\, p(r_2)\mu\left(\frac{l_1 + r_1}{L};\frac{r_2}{L}\right) \tag{3.35}$$

The equation (3.28) has to be extended by a term describing this influence. Since the roots of the motors are connected to their heads via elastic constants k and to the rest of the track via effective constants $K_e - k$, the correction in y corresponds to the x-correction attenuated by the factor k/K_e. Finally, the refined Eq. (3.29) reads

$$\langle x^n\rangle_{l_1;r_1} = \langle x\rangle - f\left(\left\langle\frac{1}{K_e}\right\rangle\frac{l_1+r_1-L}{2}+\frac{L}{k}+\frac{l_1r_1}{2\gamma}\right)+k\left\langle\frac{1}{K_e}\right\rangle\left(\langle x\rangle_{l_1+r_1;}-\langle x\rangle\right)\ . \tag{3.36}$$

The correlation to farther neighbors is still neglected. This is expressed in the simplified equation of motion which is obtained by integrating both sides of (A2) over all $\lambda_{i\geq 2}$ and $\rho_{i\geq 2}$

$$\begin{aligned}
&\frac{d}{dt}\langle x(t)\rangle\, p(\lambda_1;\rho_1) = \frac{1}{t_a}\int dl_1\int dr_1\ldots p(\ldots,l_1;r_1,\ldots) \qquad (3.37)\\
&\big[-(\langle x(t)\rangle-(fL/k)\mu\,(l_1/L;r_1/L))\,(\delta(\lambda_1-l_1)\delta(\rho_1-r_1))\\
&+(\langle x(t)\rangle-(fL/k)\mu\,(l_2/L;l_1/L))(-\delta(\lambda_1-l_2)\delta(\rho_1-l_1)+\delta(\lambda_1-l_2)\delta(\rho_1-(l_1+r_1)))\\
&+(\langle x(t)\rangle-(fL/k)\mu\,(r_1/L;r_2/L))(-\delta(\lambda_1-r_1)\delta(\rho_1-r_2)+\delta(\lambda_1-(l_1+r_1))\delta(\rho_1-r_2))\\
&+\langle x^n(t)\rangle_{l_1;r_1}\,(\delta(\lambda_1-l_1)\delta(\rho_1-r_1))\\
&+(\langle x(t)\rangle-(fL/k)\mu\,(l_2/L;(l_1+r_1)/L)\,(-\delta(\lambda_1-l_2)\delta(\rho_1-(l_1+r_1))+\delta(\lambda_1-l_2)\delta(\rho_1-l_1))\\
&+(\langle x(t)\rangle-(fL/k)\mu\,((l_1+r_1)/L;r_2/L))(-\delta(\lambda_1-(l_1+r_1))\delta(\rho_1-r_2)+\delta(\lambda_1-r_1)\delta(\rho_1-r_2))\big]\ ,
\end{aligned}$$

which leads to an integral equation for μ and v. Its scale invariant form, using the coefficient $C_2 = vt_ak/f$, is

$$\begin{aligned}
C_2 = &-3\mu(\lambda;\rho)+\int_0^\rho\mu(\lambda;\alpha)d\alpha+\int_0^\lambda\mu(\alpha;\rho)d\alpha+\left(k\left\langle\frac{1}{K_e}\right\rangle\left(\frac{\lambda+\rho-1}{2}\right)+1+\frac{\lambda\rho}{2}\frac{kL}{\gamma}\right)\\
&+k\left\langle\frac{1}{K_e}\right\rangle\int_0^\infty e^{-\alpha}\mu(\lambda+\rho;\alpha)d\alpha-(\lambda+\rho)\mu(\lambda;\rho)+\int_0^\infty e^{-\alpha}\mu(\lambda;\rho+\alpha)d\alpha+\int_0^\infty e^{-\alpha}\mu(\lambda+\alpha;\rho)d\alpha\ . \qquad (3.38)
\end{aligned}$$

A self-consistent solution that holds for all λ and ρ can be calculated numerically. The resulting coefficient C_2 is shown in Fig. 5 and a typical shape of the μ-Function in Fig. 11. The correction ν, defined in (3.32), gets the value $\nu \approx 1.50$. Taking first-order correlations into account improved the agreement between theory and simulation significantly. The remaining deviation, due to neglected correlations with further neighbors, is about 9% at low γ and lies below 14% over the entire parameter range.

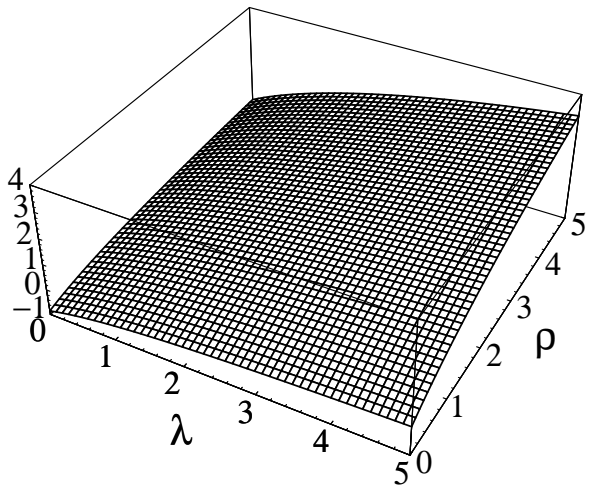

FIG. 11. The function $\mu(\lambda;\rho)$ at $\gamma/kL = 1$.

IV. STRAIN-DEPENDENT DETACHMENT RATES

A. Stiff backbone

A backbone with infinite stiffness ($\gamma\to\infty$) means that the motor roots always keep their relative positions to each other, $y_i \equiv y$ for all motors i. In this case the positions of motor roots z_i naturally play no role. The Master equation (A1) for the z-independent probability density $P(x,t)$ reduces to

$$\frac{d}{dt}P(x,t) = -r_d(x)+r_a(x) \tag{4.1}$$

with $r_d(x) = P(x)/t_a(x-y)$, $r_a(x) = \delta(x-y-d)L/\bar{L}t_d$, as follows from Eqns. (3.19-3.22). The backbone position y is determined from Eq. (3.6), summed over i:

$$k\int(x-y)P(x)dx = fL \tag{4.2}$$

Note that the norm of the distribution P gives the mean number of attached motors per length L, which, contrary to previous sections, is not necessarily equal 1. Quasistationary solutions of (4.1) are found with the ansatz

$$P(x,t) = \Phi(x-y)\ , \qquad y = vt\ , \tag{4.3}$$

leading to

$$-v\partial_\xi\Phi(\xi) = -\frac{1}{t_a(\xi)}\Phi(\xi)+\frac{L}{\bar{L}t_d}\delta(\xi-d)\ . \tag{4.4}$$

This equation is analytically solvable. For $v > 0$ the non-divergent solution is

$$\Phi(\xi) = \frac{L}{v\bar{L}t_d} \exp\left(- \int_\xi^d \frac{d\xi'}{v t_a(\xi')} \right) \theta(d-\xi) \; . \qquad (4.5)$$

Finally, the force-velocity relation can be obtained through (4.2) $f = k \int \xi \Phi(\xi) d\xi / L$. The stall force is given as

$$f(v=0) = kd \frac{t_a(d)}{\bar{L}t_d} \qquad (4.6)$$

For simplicity reasons, we model the strain-dependence of the detachment rate as an exponential function

$$t_a(\xi) = t_a \exp(\alpha \xi) \; . \qquad (4.7)$$

The form of the force-velocity-relation, which was first measured by Hill [4], is fitted perfectly with $\alpha d = 0.58$. Therefore, we use $\alpha d = 0.5$ in the following.

B. Elastic backbone

In Section III we showed that for very flexible backbones ($\gamma/kL \ll 1$) and strain-independent reaction rates ($\alpha = 0$) the zero-load velocity remains $\frac{d}{t_a}$, while the stall force is limited through the backbone stiffness as $f(v=0) = 2\gamma d/\nu L^2$. The mean strain on a motor is given as $\langle \xi \rangle = fL/k$, or $2\gamma d/\nu k L$ at maximum load. For very flexible backbones this means $\alpha \langle \xi \rangle \ll 2\alpha d \approx 1$. The strain-dependence becomes negligible and the results from Sec. III are exact. From this simple argument we expect that the force-velocity relation becomes linear. The crossover from the hyperbolic to the linear shape takes place at $\gamma/kL \approx 1$. While the stall force (force at zero velocity) $f_{\rm stall} = e^{\alpha d} kd/L$ is limited through the motor stiffness k for stiff backbones, it depends solely on the backbone stiffness for soft backbones, $f_{\rm stall} = 2\gamma d/\nu L^2$. This behavior is in agreement with our Monte-Carlo simulations, the results are shown in Fig. 6.

ACKNOWLEDGMENTS

We are grateful to Klaus Kroy, Rudolf Merkel and Erich Sackmann for helpful discussions. This work has been supported by the Deutsche Forschungsgemeinschaft under contract no. SFB 413. A.V. and E.F. would like to acknowledge support from the Cusanuswerk and by a Heisenberg fellowship from the Deutsche Forschungsgemeinschaft, respectively.

APPENDIX A: MASTER-EQUATION

In Eq. 3.17 we separated the probability density into a part depending on the distances between the z-values (l_i and r_i) and another part containing the x-positions of motors. Then we determined the attachment and detachment rates (3.19,3.20). Now we describe the temporal development of P in terms of Master equations. The detachment/attachment of one specific site leads to destruction respectively creation of the following states (see also Fig. 10):

Detachment

destroyed	created
$(\dots, l_2, l_1; x; r_1, r_2, \dots)$	
$(\dots, l_3, l_2; x_{l1}; l_1, r_1, \dots)$	$(\dots, l_3, l_2; x_{l1}; l_1 + r_1, r_2, \dots)$
$(\dots, l_1, r_1; x_{r1}; r_2, r_3, \dots)$	$(\dots, l_2, l_1 + r_1; x_{r1}; r_2, r_3, \dots)$
$\vdots$	$\vdots$

Attachment

destroyed	created
	$(\dots, l_2, l_1; x^n; r_1, r_2, \dots)$
$(\dots, l_3, l_2; x_{l1}; l_1 + r_1, r_2, \dots)$	$(\dots, l_3, l_2; x_{l1}; l_1, r_1, \dots)$
$(\dots, l_2, l_1 + r_1; x_{r1}; r_2, r_3, \dots)$	$(\dots, l_1, r_1; x_{r1}; r_2, r_3, \dots)$
$\vdots$	$\vdots$

The transition rates are given by Eqns. (3.19, 3.20). The Master equation for P is

$$
\begin{aligned}
&\frac{d}{dt}P(\xi,t)_{\dots,\lambda_2,\lambda_1;\rho_1,\rho_2,\dots}p(\dots,\lambda_1;\rho_1,\dots) = \int dx \int dl_1 \int dr_1 \dots \\
&\Big[r_d(\dots,l_2,l_1;x,t;r_1,r_2,\dots)\Big(-\delta(\xi-x)\,(\cdots\delta(\lambda_1-l_1)\delta(\rho_1-r_1)\cdots) \\
&+P(x,t)_{\dots,l_3,l_2;l_1,r_1\dots}(-\cdots\delta(\lambda_2-l_3)\delta(\lambda_1-l_2)\delta(\rho_1-l_1)\cdots+\cdots\delta(\lambda_2-l_3)\delta(\lambda_1-l_2)\delta(\rho_1-(l_1+r_1))\delta(\rho_2-r_2)\cdots) \\
&+P(x,t)_{\dots,l_1,r_1;r_2,r_3\dots}(-\cdots\delta(\lambda_2-l_1)\delta(\lambda_1-r_1)\delta(\rho_1-r_2)\cdots+\cdots\delta(\lambda_2-l_2)\delta(\lambda_1-(l_1+r_1))\delta(\rho_1-r_2)\delta(\rho_2-r_3)\cdots) \\
&\vdots \\
&\Big) \\
&+r_a(\dots,l_2,l_1;x,t;r_1,r_2,\dots)\Big(\delta(\xi-x)\,(\cdots\delta(\lambda_1-l_1)\delta(\rho_1-r_1)\cdots) \\
&+P(x,t)_{\dots,l_3,l_2;l_1+r_1,r_2\dots}(-\cdots\delta(\lambda_1-l_2)\delta(\rho_1-(l_1+r_1))\delta(\rho_2-r_2)\cdots+\cdots\delta(\lambda_1-l_2)\delta(\rho_1-l_1)\delta(\rho_2-r_1)\cdots) \\
&+P(x,t)_{\dots,l_2,l_1+r_1;r_2,r_3\dots}(-\cdots\delta(\lambda_2-l_2)\delta(\lambda_1-(l_1+r_1))\delta(\rho_1-r_2)\cdots+\cdots\delta(\lambda_2-l_1)\delta(\lambda_1-r_1)\delta(\rho_1-r_2)\cdots) \\
&\vdots \\
&\Big)\Big]
\end{aligned}
\tag{A1}
$$

Rather than in the distribution itself we are interested in the expectation value $\langle x(t)\rangle_{\dots,l_2,l_1;r_1,r_2,\dots}$. Its equation of motion follows directly form the Master equation.

$$
\begin{aligned}
&\frac{d}{dt}\langle x(t)\rangle_{\dots,\lambda_2,\lambda_1;\rho_1,\rho_2,\dots}p(\dots,\lambda_1;\rho_1,\dots) = \frac{1}{t_a}\int dl_1 \int dr_1 \dots p(\dots,l_2,l_1;r_1,r_2,\dots) \\
&\Big[-\langle x(t)\rangle_{\dots,l_2,l_1;r_1,r_2,\dots}\delta(\xi-x)\,(\cdots\delta(\lambda_1-l_1)\delta(\rho_1-r_1)\cdots) \\
&+\langle x(t)\rangle_{\dots,l_3,l_2;l_1,r_1\dots}(-\cdots\delta(\lambda_2-l_3)\delta(\lambda_1-l_2)\delta(\rho_1-l_1)\cdots+\cdots\delta(\lambda_2-l_3)\delta(\lambda_1-l_2)\delta(\rho_1-(l_1+r_1))\delta(\rho_2-r_2)\cdots) \\
&+\langle x(t)\rangle_{\dots,l_1,r_1;r_2,r_3\dots}(-\cdots\delta(\lambda_2-l_1)\delta(\lambda_1-r_1)\delta(\rho_1-r_2)\cdots+\cdots\delta(\lambda_2-l_2)\delta(\lambda_1-(l_1+r_1))\delta(\rho_1-r_2)\delta(\rho_2-r_3)\cdots) \\
&\quad\vdots \\
&+\langle x^n(t)\rangle_{\dots,l_2,l_1;r_1,r_2,\dots}\delta(\xi-x)\,(\cdots\delta(\lambda_1-l_1)\delta(\rho_1-r_1)\cdots) \\
&+\langle x(t)\rangle_{\dots,l_3,l_2;l_1+r_1,r_2\dots}(-\cdots\delta(\lambda_1-l_2)\delta(\rho_1-(l_1+r_1))\delta(\rho_2-r_2)\cdots+\cdots\delta(\lambda_1-l_2)\delta(\rho_1-l_1)\delta(\rho_2-r_1)\cdots) \\
&+\langle x(t)\rangle_{\dots,l_2,l_1+r_1;r_2,r_3\dots}(-\cdots\delta(\lambda_2-l_2)\delta(\lambda_1-(l_1+r_1))\delta(\rho_1-r_2)\cdots+\cdots\delta(\lambda_2-l_1)\delta(\lambda_1-r_1)\delta(\rho_1-r_2)\cdots) \\
&\quad\vdots \\
&\Big]
\end{aligned}
\tag{A2}
$$

This equation simplifies further if the distances l_i and r_i are distributed according to their equilibrium distribution (3.18), which is certainly the case after the motors have been running for some time.

Usually one is looking for the quasistationary solution with

$$\frac{d}{dt}\langle x(t)\rangle_{\ldots,\lambda_2,\lambda_1;\rho_1,\rho_2,\ldots} = v \ .$$

In the special case when $\langle x^n\rangle_{\ldots,l_2,l_1;r_1,r_2,\ldots}$ does not depend on l_i and r_i, the equation simplifies to (3.25). Taking first-order correlations into account but neglecting the higher ones leads to Eq. (3.37).

---

[1] B. Alberts *et al.*, *Molecular Biology of the cell*, 3 ed. (Garland Publ., New York, 1994).
[2] J. Howard, Nature **389**, 561 (1997).
[3] S. Leibler and D. Huse, J. Cell. Biol. **121**, 1357 (1993).
[4] A. Hill, Proc. R. Soc. London Ser. B **126**, 136 (1939).
[5] A. Huxley, Prog. Biophys. Biophys. Chem. **7**, 255 (1957).
[6] A. Huxley and R. Simmons, Nature **233**, 533 (1971).
[7] Y. Toyoshima *et al.*, Nature **328**, 536 (1987).
[8] J. Howard, A. Hudsepth, and R. Vale, Nature **342**, 154 (1989).
[9] K. Svoboda, C. Schmidt, B. Schnapp, and S. Block, Nature **365**, 721 (1993).
[10] J. Finer, R. Simmons, and J. Spudich, Nature **386**, 113 (1994).
[11] T. Yanagida and A. Ishijima, Biophys. J. **68**, 312s (1995).
[12] A. Ajdari and J. Prost, C.R. Acad. Sci. Paris II **315**, 1635 (1992).
[13] C. Peskin and G. Oster, Biophys. J. **68**, 202s (1995).
[14] T. Duke and S. Leibler, Biophys. J. **71**, 1235 (1996).
[15] I. Derényi and T. Vicsek, Proc. Natl. Acad. Sci. USA **93**, 6775 (1996).
[16] F. Jülicher and J. Prost, Phys. Rev. Lett. **75**, 2618 (1995).
[17] F. Jülicher, A. Ajdari, and J. Prost, Rev. Mod. Phys. **69**, 1269 (1997).
[18] Z. Csahók, F. Family, and T. Vicsek, Phys. Rev. E **55**, 5179 (1997).
[19] H. Huxley, A. Stewart, H. Sosa, and T. Irving, Biophys. J. **67**, 2411 (1994).
[20] K. Wakabayashi *et al.*, Biophys. J. **67**, 2422 (1994).
[21] H. Higuchi, T. Yanagida, and Y. Goldman, Biophys. J. **69**, 1000 (1995).
[22] J. Finer, A. Mehta, and J. Spudich, Biophys. J. **68**, 291s (1995).
[23] D. Riveline *et al.*, European Biophys. J. (1998), in press.
[24] S. Leibler, Nature **370**, 412 (1994).
[25] A. Vilfan, E. Frey, and F. Schwabl, (1997), preprint, cond-mat/9708023.
[26] A Java applet graphically visualising the simulation of our model is accessible on the internet address `http://www.physik.tu-muenchen.de/~avilfan/ecmm/`.
[27] W. Fenn, J. Physiol. (London) **184**, 373 (1924).
[28] F. Jülicher and J. Prost, Phys. Rev. Lett. **78**, 4510 (1997).
[29] A. Ishijima *et al.*, Biophys. J. **70**, 383 (1996).
[30] F. MacKintosh, J. Käs, and P. Janmey, Phys. Rev. Lett. **75**, 4425 (1995).
[31] K. Kroy and E. Frey, Phys. Rev. Lett. **77**, 306 (1996).
[32] J. Wilhelm and E. Frey, Phys. Rev. Lett. **77**, 2581 (1996).
[33] E. Frey, K. Kroy, J. Wilhelm, and E. Sackmann, Statistical Mechanics of Semiflexible Polymers: Theory and Experiments.
[34] H. Kojima, A. Ishijima, and T. Yanagida, Proc. Natl. Acad. Sci. USA **91**, 12962 (1994).
[35] D. Riveline, C. H. Wiggins, R. E. Goldstein, and A. Ott, Phys. Rev. E **56**, (1997).
[36] C. Bagshaw, *Muscle Contraction* (Chapman & Hall, London, 1993).